International Journal of Applied Mathematics

Volume 38 No. 5s, 2025

ISSN: 1311-1728 (printed version); ISSN: 1314-8060 (on-line version)

EXPERIMENTAL CHARACTERISATION OF MILLIMETRE-WAVE CHANNEL AT 28GHZ IN AN OUTDOOR ENVIRONMENT IN A NON-LINE OF SIGHT SCENARIO

Abdusalama Daho[1], Marwan Hadri Azmi[2], Dr.Razali Bin Ngah[3], Dr. Jafri bin Din[4], Dr.Asma Ali Budalal[5]

[1]Wireless Communication Centre (WCC), Faculty of Electrical Engineering, University Technology Malaysia, 81310 Skudai, Johore, Malaysia.

[2]Deputy Director of Research & Innovation, Wireless Communication Centre (WCC), School of Electrical Engineering, Universiti Teknologi Malaysia (UTM), Johor, Malaysia.

[3]Wireless Communication Centre (WCC), Faculty of Electrical Engineering, Universiti Teknologi Malaysia, 81310, UTM Skudai, Johor Bahru

[4]Faculty of Electrical and Electronic Engineering, Universiti Teknologi Malaysia (UTM), Malaysia

[5]College of Electrical and Electronics Technology, Benghazi, Libya

E-mail: ibabdusalama2@graduate.utm.my[1], hadri@utm.my[2], razalingah@utm.my[3], asma.budalal@ceet.edu.ly[5]

Abstract

The present study provides an experimental characterisation of a millimetre-wave (mm-W) channel at a frequency of 28GHz for an outdoor environment with a non-line of sight (NLOS) scenario. The channel sounder system (CSS) correlation was employed to record the channel response, and the power delay profile (PDP) and path loss values were measured [1]. For vertically polarised antenna configurations, RMS delay spread across the band was employed along with a highly directional horn receiver antenna as well as an omnidirectional transmitter antenna. We considered a typical urban threshold of 10dB and an urban threshold of 20dB for areas operating at 28GHz frequency. The measurements for 10dB and 20dB urban threshold environments considered the values of path loss exponent (n) use models: cost-231 (CI) and free space (FI) [2]. The path loss was compared and analysed with regard to the 10dB and 20dB measured urban threshold data. As per the results pertaining to this research, for 10 dB urban threshold areas, the path loss estimation had an observed impact as distance increased. At the start of the measurements pertaining to the 10dB urban threshold environment, the losses were found to be around 112dB post 110m distance from the measurement survey. The measurement analysis anticipates normal signal quality near the collector set for the specified removal from the transmitter and also the variation in the signal quality with regard to the specific environment. The results based on this work are regarded as beneficial for planning and installation of any base station in similar environments or locations. These outcomes provide rules for arranging cells in remote communication

Received: August 02, 2025

Volume 38 No. 5s, 2025
ISSN: 1311-1728 (printed version); ISSN: 1314-8060 (on-line version)

frameworks since path loss is important for calculations within the plan pertaining to any radio communications framework system [3].

Keywords: 5G, Mm-wave, outdoor environment, 28GHz, tropical region, threshold.

1. Introduction

The introduction sets the stage for understanding the experimental characterisation of millimetre-wave (mm-W) channels at 28GHz in a non-line-of-sight (NLOS) scenario. With the recent surge in interest in mm-W systems, there is a growing need to address the challenges posed by unfavourable wireless propagation in these settings. This includes innovative approaches to physical layer system design to mitigate impairments. Notably, beamforming with a large number of antennas is crucial for meeting the link margin of mm-W systems. Additionally, there is a strong focus on comprehending radio frequency (RF) design challenges for large bandwidth systems, as well as measurements and channel modelling at different carrier frequencies of interest [1].

Furthermore, this work describes the experimental setup for 5G operation at 28GHz and 60GHz in an urban environment, including outdoor and indoor details. The study also highlights the use of omnidirectional and highly directional antennas for transmission and reception, as well as the consideration of different beamwidth values for potential coverage areas. This scenario allows for the study of urban microcells (UMI), indoor WLAN-based femtocells, and proposed intelligent transportation system use cases, such as inter-car, intra-car, and infrastructure-to-infrastructure communications [2].

2. Background and Significance

Recent attention to mm-W systems has sparked a growing interest in understanding the channel characteristics and implications for physical layer design [1]. The unfavourable wireless propagation in mm-W settings necessitates innovative approaches, with beamforming and a large number of antennas playing a key role in meeting the link margin of mm-W systems. Studies have shown that losses at mm-W frequencies are typically higher than with sub-6GHz systems in both indoor and outdoor settings, with significant increases in delay spreads observed in outdoor scenarios. Additionally, the impact of reflection response and penetration through walls of residential buildings has been studied, revealing a significant loss of coverage at mm-W frequencies corresponding to deep frequency notches.

In a related study, measurements were performed using omnidirectional and highly directional antennas to analyse the 5G operation at 28GHz and 60GHz in urban environments, including full building and outdoor details [2]. The scenario was designed to study urban microcells (UMI) and indoor WLAN-based femtocells and proposed intelligent transportation systems use cases, demonstrating the potential for adequate communication capabilities within urban canyons.

Received: August 02, 2025

International Journal of Applied Mathematics

Volume 38 No. 5s, 2025

ISSN: 1311-1728 (printed version); ISSN: 1314-8060 (on-line version)

3. Materials and Methods

Measurement Equipment

The wideband channel sounder system (CSS) was employed for measurement. Figure 1 demonstrates the measurement equipment. An E8267D up-converter, an M8190A arbitrary waveform generator, and an FS725 rubidium clock are included in CSS Tx.

The wideband differential in-phase quadrature (IQ) is produced by M8190A, i.e., arbitrary waveform channel sounding (AWCS) signals, which gave 1ns multipath resolution based on a 1000Mcps pseudo-random binary sequence (PRBS). The IQ is up-converted by E8267D into RF (up to 40GHz), wherein the output adjustment is performed using the automatic line controller circuit of the E8267D. FS725 synchronised the Rx and Tx by considering a 10MHz reference (<3e-11 stability; <le-11 accuracy) [4]. The signals have been derived based on FS725 or 33500B function generation. The AWCS chip rate was found to be 1000Mcps, which produced a 1GHz AWCS signal. To emulate the hotspot location, Tx antennas were positioned at a height of 1.7m, and Rx was positioned at a height of 1.5m.

The RF (up to 40GHz) was down-converted by M9362AD01 Rx to an intermediate frequency, which was amplified by M9352A and captured by a 12-bit M9703A digitiser having a 1GHz bandwidth. The local oscillator pertaining to M9362A-D01 signified EXG N5173B analogue signal, while M9300A presented a frequency reference mode, along with external 10MHz and 100MHz references. Rx FS725 provided a 10MHz reference, and the signal was loaded via a 33500B. This research work employed horn and omnidirectional antennas.

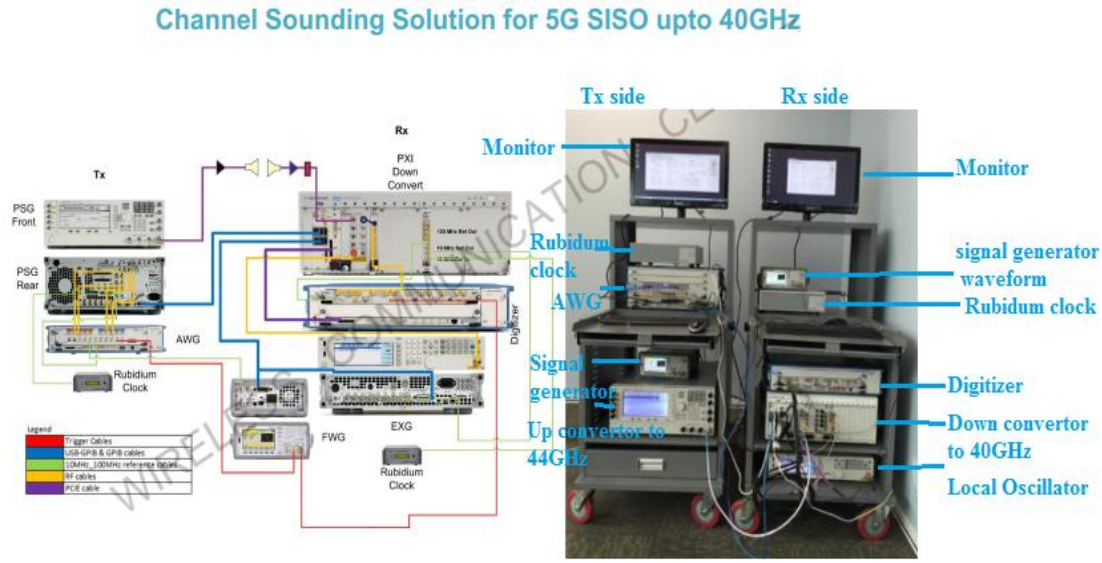

Figure 1. The 5G CSS

Received: August 02, 2025

International Journal of Applied Mathematics

Volume 38 No. 5s, 2025

ISSN: 1311-1728 (printed version); ISSN: 1314-8060 (on-line version)

Measurement Campaign

Outdoor NLOS scenario.

Measurement Set Up

Measurements were taken at the UTM-KL grounds in an outdoor roadside setting next to the PA building (Figure 2). A 15dB power amplifier operating at 28 GHz was used to amplify the 25dBm signal. An 11.6-horn antenna was used to transmit the signal. The backroad near the PA block was used as a Tx antenna location, and a 1.7m tripod was used to mount the antenna. A low noise amplifier omnidirectional antenna with 24.5dBi gain was mounted at 1.7m for the receiver. Tx antenna position was static. On the other hand, the Rx antenna was tested using 10 points that faced obstruction from the PA building corner with respect to the Tx antenna. Rx measurements with distance are specified in the table, which also specifies NLOS characteristics for -20 and -10dB thresholds. All Tx-Rx points were tested using several azimuth angles to optimise incident power [5].

Figure 2. The measurement environment for the NLOS scenario

Table 1. The NLOS parameters at -20dB and -10dB thresholds

Freq. (GHz)	Distance (m)	High of Tx Antenna (m)	High of Rx Antenna (m)	Pol.	Pt	Pr	CI Model 1m,3m,5m -20dB Threshold		FI Model -20dB Threshold		
							PLE (*n*)	σ (dB)	α (dB)	β	σ (dB)
28	20	1.5	1.5	V-V			2.4	3.0	58.6	2.6	3.0
28	30	1.5	1.5	V-V			1.9	3.2	58.4	2.5	1.4
28	40	1.5	1.5	V-V			1.6	3.3	58.6	2.6	3.0
28	50	1.5	1.5	V-V			2.3	1.4	58.4	2.5	1.4

Received: August 02, 2025

International Journal of Applied Mathematics

Volume 38 No. 5s, 2025

ISSN: 1311-1728 (printed version); ISSN: 1314-8060 (on-line version)

28	60	1.5	1.5	V-V			1.8	1.5	58.4	2.5	1.4
28	70	1.5	1.5	V-V			1.6	1.7	58.4	2.5	1.4
Freq. (GHz)	Distance (m)	High of Tx Antenna (m)	High of Rx Antenna (m)	Pol.	Pt	Pr	CI Model 1, 3, and 5m -10dB Threshold		FI Model -10dB Threshold		
28	80	1.5	1.5	V-V			**PLE (*n*)**	**σ (dB)**	**α (dB)**	**β**	**σ (dB)**
28	80	1.5	1.5	V-V			2.4	4.7	62.6	2.4	4.7
28	90	1.5	1.5	V-V			1.9	4.8	62.6	2.4	4.7
28	90	1.5	1.5	V-V			1.7	5.0	62.6	2.4	4.7
28	100	1.5	1.5	V-V			2.5	1.4	60.6	2.5	1.4
28	110	1.5	1.5	V-V			1.9	1.5	60.6	2.5	1.4
28	110	1.5	1.5	V-V			1.7	1.6	60.6	2.5	1.4

4. Results and Discussions

Figure 3 depicts path loss characteristics between 90 and 112dB for 10 distinct receivers mounted within 20 to 110m of the transmitter when tested at a 20dB limit. Visual assessment at the specified points (receiver points in blue colour and transmitter points in yellow colour) indicated that more distance was associated with a higher path loss. Two popular approaches (cost-231 (CI) and free space (FI) models) were used to fit experimental data. The CI path loss approach used three particular scenarios (d0=1, 3, and 5m). Path loss exponent (n) measurements for 1, 3, and 5m distance were ascertained as 2.4, 1.9, and 1.6, respectively. The optimal measurement fit for the CI approach concerning the 1m reference separation is depicted in Figure 3 using a red dash-dot notation. The FI approach for path loss measurement had a 2.6 slope value (β denotes the n) for an intercept α=58.6 dB, which is lower than the 2.7dB theoretical reference for 1m and 28GHz. The CI and FI model agreement is optimised for a 1m distance. The alignment is clear for the FI and CI model parameters. The 1m CI model n is 0.2 units less than the FI model slope value. Both approaches have identical standard deviations (σ=3 dB) [5].

Received: August 02, 2025

International Journal of Applied Mathematics

Volume 38 No. 5s, 2025

ISSN: 1311-1728 (printed version); ISSN: 1314-8060 (on-line version)

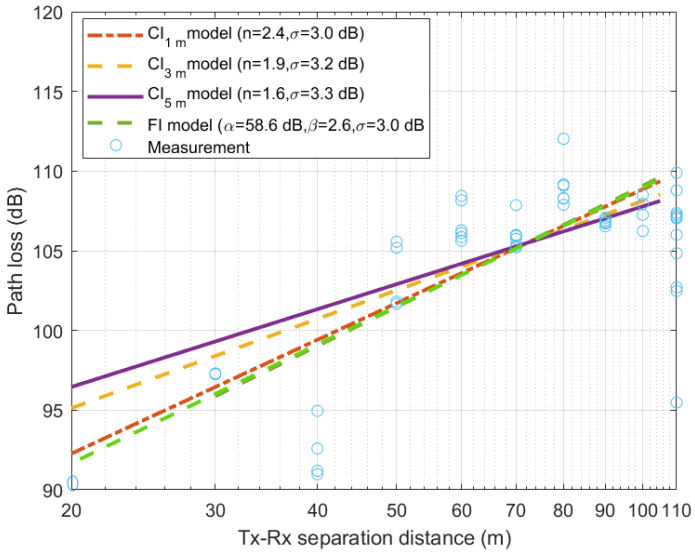

Figure 3. The path loss in relation to the Tx-Rx separation distance using the 20dB threshold

Figure 4 presents path loss changes between 90 and 119 dB for 10 receivers having between 20 and 110m transmitter distance, measured using the 10dB limit. Two popular approaches (CI and FI models) were used to fit experimental data. The CI path loss approach used three particular scenarios (d0=1, 3, and 5m). Path loss exponent (n) measurements for 1, 3, and 5m distance were ascertained as 2.4, 1.9, and 1.7, respectively. Concerning the 20dB limit outcomes, the optimal measurement fit for the 10dB limit is the CI approach for 1m separation (n=2.4), as depicted in Figure 5 using the red dash-dot notation. The FI approach for path loss measurement had a 2.4 slope value (β denotes the n) for an intercept α=62.2dB, which is higher by 0.9dB than the theoretical reference for 1m and 28GHz. The 1m CI approach is aligned with the FI model for data fitment using identical parameters, i.e., n and σ of 2.4 and 4.7dB, respectively. Contrasting the outcomes of the -10 and -20dB limit path loss parameters, we present the average values for every limit and path loss approach in Figure 4.3.

The plot indicates path loss averages between 90 and 109dB for 20dB and 94.6 and 112.5dB for 10dB limits. Figure 6 indicates that the 10dB model has a higher average path loss than the 20dB model for most points. The maximum difference between average values is 10dB despite the varying path loss averages. The 40m transmitter-receiver distance measurement for the 10dB limit is 102.3dB higher than the 92.4dB path loss by 9.9dB for the 20dB limit. In the 20dB limit context, the CI approach considers average n measurements as 2.3, 1.8, and 1.6 with corresponding σ=1.4, 1.5, and 1.7dB for 1, 3, and 5m distance. Considering the 10dB limit, the n change to 2.5, 1.9, and 1.7 with corresponding σ=1.4, 1.5, and 1.6dB for 1, 3, and 5m separation. The CI model path loss parameter for the 10dB limit and 1m distance exceeds the 20dB value by 0.2 (representing 2dB every decade).

The two thresholds have identical slope values of 2.5 and σ=1.4 dB measured using the FI model. The intercepts differ by a maximum of 2.2dB (α=60.6dB and 58.4dB for -10 and -

Received: August 02, 2025

International Journal of Applied Mathematics

Volume 38 No. 5s, 2025

ISSN: 1311-1728 (printed version); ISSN: 1314-8060 (on-line version)

20dB limits, respectively). The 10dB limit has an FI intercept superior to the 20dB measurement based on the 28GHz free space path loss constant for 1m separation. Figures 4-6 suggest that the CI approach for 1m reference separation (CI1m) and the FI approach optimally fit the NLOS outdoor scenario using -10 and 20dB limits at 28GHz. The 10dB limit might be employed in place of the suggested 20dB limit for identical 20dB observations. This NLOS assessment indicates that 10dB presents reduced time and complexity for determining channel characteristics without compromising path loss efficacy [6].

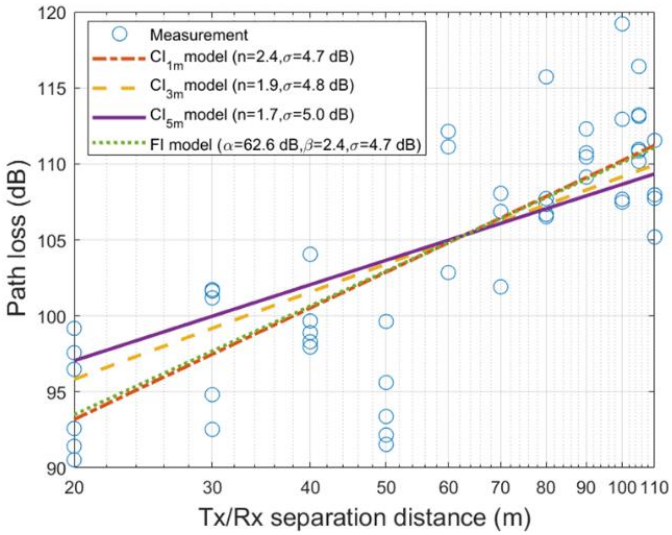

Figure 4. The path loss in relation to the Tx-Rx separation distance using the 10dB threshold

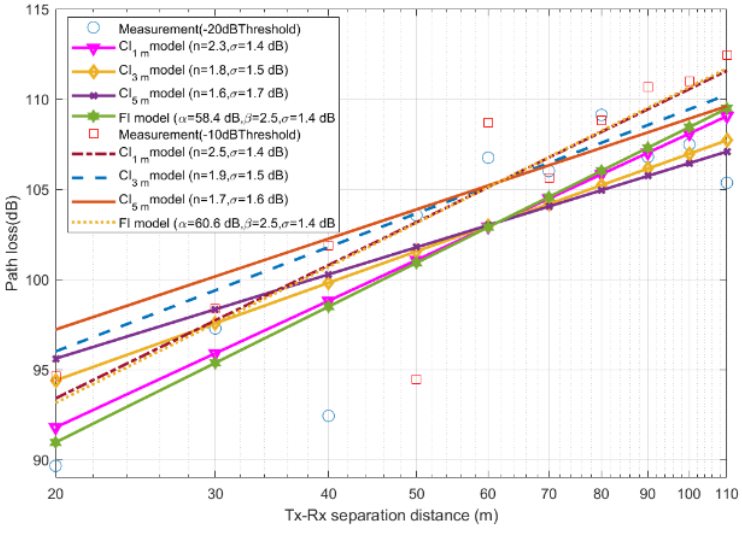

Figure 5. A comparison of the path losses using the -10 and -20dB thresholds

Figures 6 and 7 display the power delay profiles (PDP) for the 80 and 90m Tx-Rx separation distances as regards actual propagation time delay at the -10 and -20dB thresholds. For a PDP of 80m, Figure 6 indicates that at the -20dB threshold, the total of multipath

Received: August 02, 2025

International Journal of Applied Mathematics
Volume 38 No. 5s, 2025
ISSN: 1311-1728 (printed version); ISSN: 1314-8060 (on-line version)

components (MPCs) is 20 and five dominant paths will appear at the 10dB threshold. The remaining 15 MPCs are lost once the -10dB threshold is applied. The five dominant paths show respective powers of -120.5, -119.8, -119.8, -120.6, and -110.8dB, corresponding to propagation time delays of 687, 707, 751, 752, and 753ns.

It is worth mentioning that maximum power becomes available in the newest of these five dominant paths in this Rx location. Notably, even these 15 MPCs are lost at the 10dB threshold in the scenario for the 80m Rx location, resulting in an average path loss of 109.1dB. This value is close to the path loss of 108.8dB observed at the 20dB threshold (Figure 5). This suggests that the non-dominant paths which appear at the 20dB threshold all contribute power at a low level to the total received. Another evident result is that the dominant-path maximum is not required for such arrival in early access, for this relies on Rx location and not Tx-Rx distance, as shown for 90m in the next figure. It implies that MPC propagation time delay is dependent on the available physical objects surrounding the Rx antenna.

Figure 7 displays the PPD versus propagation time delay for the 90m Tx-Rx distance. Clearly, every dominant path in this Rx location exhibits early access. It follows that every dominant MPC has been received with a propagation delay lower than 683ns. For this location, the total number of MPCs is also 20 paths, which equals the total number of MPCs for 80m. Nevertheless, the total number of dominant paths is seven MPCs, with all received at the -20 and -10dB thresholds. Despite the fact that 13 MPCs are lost at the 10dB threshold, Figure 5 shows the average path loss in the 90m Rx location as 110.7dB. This is higher by only 3.9dB than the mean path loss of 106.8dB as recorded at the 20dB threshold. Remarkably, propagation time delay for 90m reaches a maximum of 800ns even though most MPCs arrived in early access at the Rx. The maximum propagation time delay for 80m is 759ns, even though the majority of dominant paths are received in late access.

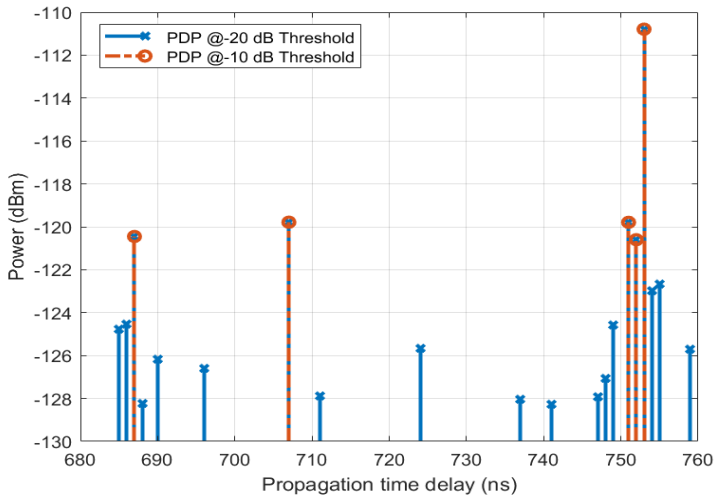

Figure 6. The PDP in terms of the propagation time delay using the -10 and -20dB thresholds at a Tx-Rx separation distance of 80m

Received: August 02, 2025

International Journal of Applied Mathematics

Volume 38 No. 5s, 2025

ISSN: 1311-1728 (printed version); ISSN: 1314-8060 (on-line version)

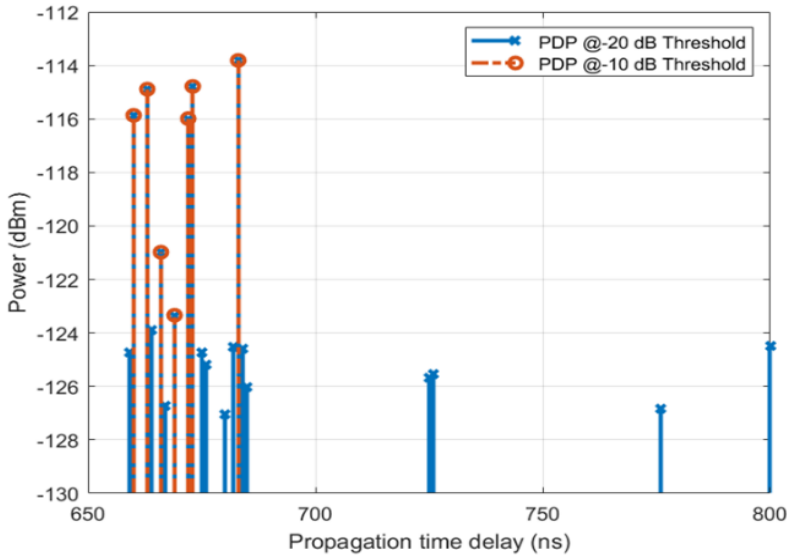

Figure 7. The PDP in terms of the propagation time delay using the -10 and -20dB thresholds at a Tx-Rx separation distance of 90m

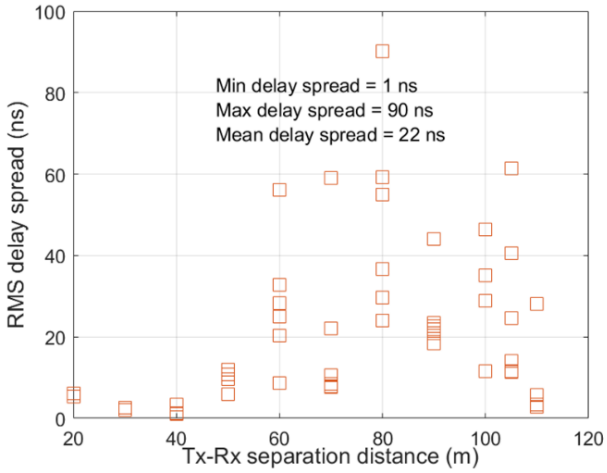

Figure 8. The RMS delay using the 20dB threshold along the Tx-Rx separation distance

Received: August 02, 2025

International Journal of Applied Mathematics
Volume 38 No. 5s, 2025
ISSN: 1311-1728 (printed version); ISSN: 1314-8060 (on-line version)

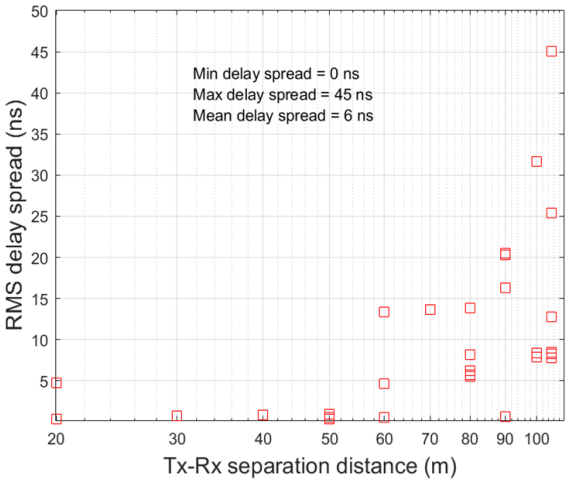

Figure 9. The RMS delay using the 10dB threshold along the Tx-Rx separation distance

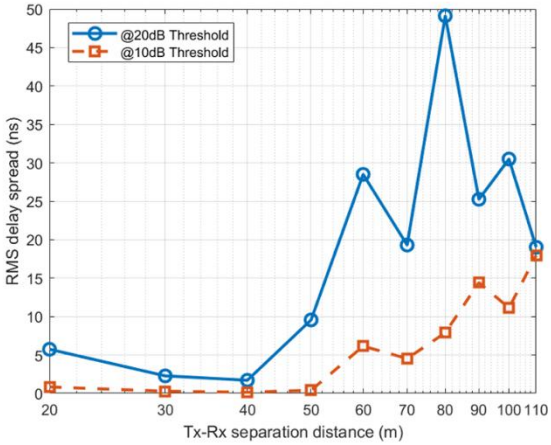

Figure 10. The average RMS delay using the 10dB threshold along the Tx-Rx separation distance

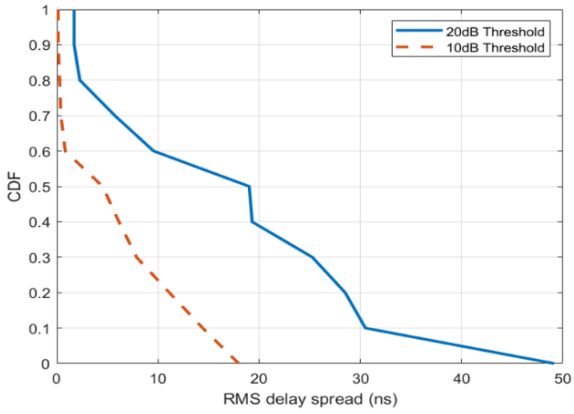

Figure 11. The CDF of the average RMS delay using the -10 and -20dB thresholds

4.1. Results

Received: August 02, 2025

Volume 38 No. 5s, 2025
ISSN: 1311-1728 (printed version); ISSN: 1314-8060 (on-line version)

The present study analysed path loss and delay in an outdoor NLOS scenario at 28GHz. The key findings were:

Model and Method

- **Path Loss Models:** The CI and FI path loss models were used to fit the measured data. Different reference distances (d0=1, 3, and 5m) were used for the CI model.
- **Threshold Selection:** The study compares the results using -10 and -20dB thresholds for identifying MPCs in the PDP.

Scenario

- **Outdoor NLOS Environment:** The measurements were conducted in a roadside environment within the UTM-KL campus, utilising a 1.7m tripod for both the transmitter and receiver antennas.
- **Frequency:** 28GHz

Technical Results

- **Path Loss:** The CI model with a 1m reference distance showed the best fit for the data, with an n of around 2.4 for both -10 and -20dB thresholds.
- **Delay Spread:** The RMS delay spread increases with increasing Tx-Rx separation distance, reaching up to 90ns at -20dB threshold and 45ns at -10dB threshold.
- **Threshold Comparison:** While the -20dB threshold provides a larger number of MPCs, the -10dB threshold offers a good compromise in terms of path loss performance and complexity.
- **Dominant Paths:** MPCs (paths with the highest power) are received earlier than the weaker ones, even when a significant number of MPCs are lost due to thresholding.

4.2. Discussion

The present study demonstrated that:

- **Accurate Path Loss Estimation:** The CI model with a 1m reference distance provides a good fit for the path loss in the outdoor NLOS environment at 28GHz.
- **Threshold Impact:** Thresholding significantly impacts the number of MPCs detected, but the average path loss and delay spread characteristics can still be reasonably well estimated even with a lower threshold.
- **Dominant Path Significance:** Dominant paths are crucial for signal reception, and their arrival time significantly influences the overall channel performance.
- **Future Applications:** These findings provide valuable insights for designing future wireless communication systems operating in NLOS environments at mm-W frequencies.

Overall, the present study provides a comprehensive analysis of path loss and delay spread

Received: August 02, 2025

International Journal of Applied Mathematics

Volume 38 No. 5s, 2025

ISSN: 1311-1728 (printed version); ISSN: 1314-8060 (on-line version)

in an outdoor NLOS scenario at 28GHz, contributing valuable data for future research and system design in this frequency band.

The choice between the -10 and -20dB thresholds depends on the context and the specific application under consideration. The selected threshold level determines when a signal will be considered significant enough to trigger an action or response in various audio, signal processing, or measurement scenarios. A breakdown of both options is provided below:

- **-10dB Threshold:** A threshold of -10dB is higher than -20dB counterpart, meaning it's a less sensitive threshold. This means that a signal would need to be stronger or louder to cross the -10dB threshold and trigger a response. Choosing a -10dB threshold could be appropriate when it is desirable to filter out smaller or less significant variations in a signal, allowing only relatively stronger events to trigger a response. This is often used in noise reduction or dynamic range compression situations where low-level background noise must be ignored.

- **-20dB Threshold:** A threshold of -20dB is lower than -10dB, making it a more sensitive threshold. In this case, even weaker or quieter signals would be able to cross the threshold and trigger a response. This can be useful when it is desirable to capture a wider range of events, including those that might be quieter or less pronounced. It is often used in applications where the situation requires more inclusion of lower-level signals, such as in some types of audio processing where subtle details or effects need to be captured.

Ultimately, the best threshold depends on the specific goals and requirements. If the aim is to strike a balance between sensitivity and filtering noise, a threshold (like -15dB) may be considered. It is important to consider the characteristics of the signals being worked with, the level of noise in the system, and the desired outcome to make an informed decision about the appropriate threshold [7].

5. Conclusion

This study introduced the NLOS n propagation features of the 5G channel at specific 28GHz frequency bands. Dual schemes have been proposed to examine the losses that result from threshold as well as high-frequency band operation. Wideband measurements were carried out at 28GHz with the use of a 5G CSS featuring a high chip processing rate of 1000Mbps. Various 5G channel parameters for the excess delay, path loss, and PDP were determined. Signal loss at the 10dB and 20dB thresholds and high frequency was studied. Path loss exponent (n) values in the NLOS scenario at the 10dB threshold for CI and FI n, and also at the 20dB threshold for CI and FI, shown, with differences corresponding to 1.6 and 1.3 at 3.5 and 28GHz, respectively. Nevertheless, received power dropped in the NLOS scenario [8] with PLE values corresponding to 2.7 and 3.6 at 3.5GHz and 28GHz, respectively. The 3GPP models, namely FI and ABG, delivered reliable performance despite path loss for multi-frequency and single models in the LOS scenario. According to the proposed models, mean diffraction loss values correspond to 11.11 and 23.37dB at 3.5GHz and 28GHz, respectively. The loss resulting in terms of frequency drop was 19.73dB in the LOS scenario

Received: August 02, 2025

Volume 38 No. 5s, 2025
ISSN: 1311-1728 (printed version); ISSN: 1314-8060 (on-line version)

and 32.00dB in the NLOS scenario. RMS delay values were correspondingly lower than 8 and 12ns in the LOS and NLOS scenarios, respectively, for both frequency bands. These results imply that the 5G channel offers good performance potential in terms of path loss and the advantage of exceptionally low delay spread. The results of this study will be useful for testing and implementation in real environments and should provide insight into next-generation IoT-driven smart city 5G networks. The findings also suggest that 5G wireless networks of the future can support higher data rates with lower latencies, using highly directive antennae that deliver high gain power through small-size cells [9-22].

Acknowledgements

The authors would like to thank the Wireless Communication Centre at Universiti Teknologi Malaysia for providing the necessary equipment and facilities for this research. The authors are also grateful to the research participants for their time and effort. The authors would also like to acknowledge the support of the anonymous reviewers for their insightful comments and suggestions, which helped to improve the quality of the manuscript.

Conflicts of Interest

The authors declare no conflict of interest.

References

[1] R. Vasanthan, A. Partyka, L. Akhoondzadeh-Asl, M. A. Tassoudji, O. H. Koymen and J. Sanelli, "Millimeter wave channel measurements and implications for PHY layer design," *IEEE Transactions on Antennas and Propagation,* vol. 65, no. 12, pp. 6521-6533, Dec 2017.

[2] L. Azpilicueta, P. Lopez-Iturri, J. Zuñiga-Mejia, M. Celaya-Echarri, F. A. Rodriguez-Corbo, C. Vargas-Rosales, E. Aguirre, D. G. Michelson and F. Falcone, "Fifth-generation (5G) mmWave spatial channel characterization for urban environments' system analysis," *Sensors,* vol. 20, no. 18, p. 5360, Sep 2020.

[3] A.M. Daho, T. A. Rahman, A. M. Al-Samman and Y. Yamada, "Survey study on outdoor wideband system propagation of millimeter wave at 28-ghz in a 5g network system," *International Journal of Engineering and Technology,* vol. 7, no. 4, pp. 6810-6821, Apr 2018.

[4] M. Al-Samman, M. H. Azmi and T. A. Rahman, "A survey of millimeter wave (mm-Wave) communications for 5G: Channel measurement below and above 6 GHz," in *Recent Trends in Data Science and Soft Computing (IRICT 2018)*, Kuala Lumpur, Malaysia, 2019.

[5] M. Al-Samman, T. A. Rahman, T. Al-Hadhrami, A. Daho, M. N. Hindia, M. H. Azmi, K. Dimyati and M. Alazab, "Comparative study of indoor propagation model below and above 6 GHz for 5G wireless networks," *Electronics,* vol. 8, no. 1, p. 44, Jan 2019.

[6] M. Daho, Y. Yamada, A. M. Al-Samman, T. A. Rahman, M. H. Azmi and A. Arsad, "Proposed path loss model for outdoor environment in tropical climate for the 28-GHz 5G system," in *1st International Conference on Emerging Smart Technologies and*

Received: August 02, 2025

Volume 38 No. 5s, 2025

ISSN: 1311-1728 (printed version); ISSN: 1314-8060 (on-line version)

Applications (eSmarTA), Sana'a, Yemen, 2021.

[7] A. H. Budalal, M. R. Islam, K. Abdullah and T. A. Rahman, "Modification of distance factor in rain attenuation prediction for short-range millimeter-wave links," *IEEE Antennas and Wireless Propagation Letters,* vol. 19, no. 6, pp. 1027-1031, Jun 2020.

[8] A. Budalal, I. Shayea, M. R. Islam, M. H. Azmi, H. Mohamad, S. A. Saad and Y. I. Daradkeh, "Millimetre-wave propagation channel based on NYUSIM channel model with consideration of rain fade in tropical climates," *IEEE Access,* vol. 10, pp. 1990-2005, Jan 2022.

[9] U. C. Bas, R. Wang, S. Sangodoyin, S. Hur, K. Whang, J. Park, J. Zhang and A. F. Molisch, "28 GHz propagation channel measurements for 5G microcellular environments," in *International Applied Computational Electromagnetics Society Symposium (ACES)*, Denver, CO, USA, 2018.

[10] W. A. Gulzar Khawaja, Ö. Özdemir, F. Erden, I. Guvenc, M. Ezuma and Y. Kakishima, "Effect of passive reflectors for enhancing coverage of 28 GHz mmWave systems in an outdoor setting," in *IEEE Radio and Wireless Symposium (RWS)*, Orlando, Florida, USA, 2019.

[11] W. A. Gulzar Khawaja, Ö. Özdemir, Y. Yapici, I. Guvenc and Y. Kakishima, "Coverage enhancement for mm wave communications using passive reflectors," in *11th Global Symposium on Millimeter Waves (GSMM)*, Boulder, CO, USA, 2018.

[12] S. Kumar, S. A. Rao and N. Kumar, "Modeling and link budget estimation of directional mmwave outdoor environment for 5G," in *European Conference on Networks and Communications (EuCNC)*, Valencia, Spain, 2019.

[13] J.-H. Lee, J.-S. Choi, J.-Y. Lee and S.-C. Kim, "28 GHz millimeter-wave channel models in urban microcell environment using three-dimensional ray tracing," *IEEE Antennas and Wireless Propagation Letters,* vol. 17, no. 3, pp. 426-429, Mar 2018.

[14] S. Li, Y. Liu, L. Leke, X. Sun, S. Yang and D. Sun, "Millimeter-wave channel simulation and statistical channel model in the cross-corridor environment at 28 GHz for 5G wireless system," in *International Conference on Microwave and Millimeter Wave Technology (ICMMT)*, Chengdu, China, 2018.

[15] M. B. Majed, T. A. Rahman and O. A. Aziz, "Propagation path loss modeling and outdoor coverage measurements review in millimeter wave bands for 5G cellular communications," *International Journal of Electrical and Computer Engineering (IJECE),* vol. 8, no. 4, p. 2254–2260, Aug 2018.

[16] F. Qamar, M. N. Hindia, K. Dimyati, K. A. Noordin, M. B. Majed, T. A. Rahman and I. S. Amiri, "Investigation of future 5G-IoT millimeter-wave network performance at 38 GHz for urban microcell outdoor environment," *Electronics ,* vol. 8, no. 5, p. 495, May 2019.

[17] F. Qamar, M. N. Hindia, T. Abbas, K. Dimyati and I. S. Amiri, "Investigation of QoS performance evaluation over 5G network for indoor environment at millimeter wave bands," *International Journal of Electronics and Telecommunications,* vol. 65, no. 1, pp. 95-101, Feb 2019.

Received: August 02, 2025

Volume 38 No. 5s, 2025

ISSN: 1311-1728 (printed version); ISSN: 1314-8060 (on-line version)

[18] F. Qamar, M. H. S. Siddiqui, M. N. Hindia, K. Dimyati, T. A. Rahman and M. S. A. Talip, "Propagation channel measurement at 38 GHz for 5G mm-wave communication network," in *IEEE Student Conference on Research and Development (SCOReD)*, Selangor, Malaysia, 2018.

[19] J. D. V. Sánchez, L. Urquiza-Aguiar and M. C. P. Paredes, "Fading channel models for mm-wave communications," *Electronics ,* vol. 10, no. 7, p. 798, Mar 2021.

[20] R. Asif, "Design and implementation of system components for radio frequency based asset tracking devices to enhance location based services," Ph.D. dissertation, Faculty of Engineering and Informatics, University of Bradford, Bradford, UK, 2017.

[21] W. Manan, H. A. Obeidat, A. Alabdullah, R. Abd-Alhameed and F. Hu, "Indoor to indoor and indoor to outdoor millimeter wave propagation channel simulations at 26 Ghz, 28 Ghz and 60 Ghz for 5G mobile networks," *The International Journal of Engineering and Science (IJES),* vol. 7, no. 3, pp. 8-18, Mar 2018.

[22] W. Manan, H. A. Obeidat, A. Alabdullah, R. Abd-Alhameed and F. Hu, "Indoor to indoor and indoor to outdoor millimeter wave propagation channel simulations at 26 Ghz, 28 Ghz and 60 Ghz for 5G mobile networks," *The International Journal of Engineering and Science (IJES),* vol. 7, no. 3, pp. 8-18, Mar 2018.

[23] E. M. Vitucci, V. Degli-Esposti, F. Mani, F. Fuschini, M. Barbirolli, M. Gan, C. Li, J. Zhao and Z. Zhong, "Tuning ray tracing for mm-wave coverage prediction in outdoor urban scenarios," *Radio Science,* vol. 54, no. 11, pp. 1112-1128, Nov 2019.

Received: August 02, 2025